Fracture-controlled fluid transport supports microbial methane-oxidizing communities at the Vestnesa Ridge

Haoyi Yao[1], Wei-Li Hong[1,2], Giuliana Panieri[1], Simone Sauer[1,2], Marta E. Torres[3], Moritz F. Lehmann[4], Friederike Gründger[1] and Helge Niemann[1,4,5,6]

[1]CAGE - Centre for Arctic Gas Hydrate, Environment and Climate, Department of Geosciences, UiT The Arctic University of Norway in Tromsø, Norway
[2]NGU-Geological Survey of Norway, Trondheim, Norway
[3]CEOAS- College of Earth, Ocean, and Atmospheric Sciences, Oregon State University, Corvallis, USA
[4]Department of Environmental Sciences, University of Basel, Switzerland
[5]NIOZ Royal Netherlands Institute for Sea Research, Department of Marine Microbiology and Biogeochemistry, and Utrecht University, The Netherlands
[6]Faculty of Geosciences, Department of Earth Sciences, Geochemistry, Utrecht University, The Netherlands

Correspondence to: Haoyi Yao (haoyi.yao@uit.no)

Abstract. We report a rare observation of a mini-fracture in near-surface sediments (30 cm below the seafloor) visualized using rotational scanning X-ray of a core recovered from the Lomvi pockmark, Vestnesa Ridge west of Svalbard (1200 m water depth). Porewater geochemistry and lipid biomarker signatures revealed clear differences in the geochemical and biogeochemical regimes of this core compared with two additional unfractured cores recovered from pockmark sites at Vestnesa Ridge, which we attribute to differential methane transport mechanisms. In the sediments core featuring the shallow mini-fracture at pockmark Lomvi, we observed high concentrations of both methane and sulfate throughout the core in tandem with moderately elevated values for total alkalinity, ^{13}C-depleted dissolved inorganic carbon (DIC), and ^{13}C-depleted lipid biomarkers (diagnostic for the slow-growing microbial communities mediating the anaerobic oxidation of methane with sulfate - AOM). In a separate unfractured core, recovered from the same pockmark about 80 m away from the fractured core, we observed complete sulfate depletion in the top centimeters of the sediment and much more pronounced signatures of AOM than in the fractured core. Our data indicate a gas advection-dominated transport mode in both cores facilitating methane migration into sulfate-rich surface sediments. However, the moderate expression of AOM signals suggest a rather recent onset of gas migration at the site of the fractured core, while the geochemical evidence for a well-established AOM community at the second coring site suggest that gas migration has been going on for a longer period of time. A third core recovered from another pockmark along the Vestnesa Ridge, Lunde pockmark, was dominated by diffusive transport with only weak geochemical and biogeochemical evidence for AOM. Our study highlights that advective fluid and gas transport supported by mini-fractures can be important in modulating methane dynamics in surface sediments.

1 Introduction

Large-scale fractures are commonly observed on seismic profiles (Tobin et al., 2001;Weinberger and Brown, 2006;Plaza-Faverola et al., 2015) and can provide increased sediment permeability and conduits for fluid/gas transport. Macro-fractures

were often observed in association with cold seep systems, where methane-rich fluids from greater sediment depth reach shallow sediments and may even be transported across the sediment-water-interface (Berndt et al., 2014;Sahling et al., 2014). Prominent examples of fracture-controlled fluid migration at cold seep systems include locations such as Hydrate Ridge (Torres et al., 2002;Weinberger and Brown, 2006;Briggs et al., 2011), Blake Ridge (Egeberg and Dickens, 1999) and the recently documented Storfjordrenna gas hydrate mounds in the Barents Sea(Hong et al., 2017b;Hong et al., 2018;Waage et al., 2019). Seepage at these locations can sustain high biomass of chemosynthetic communities that either directly oxidize methane, or metabolize products of methane oxidation, such as sulfide (Boetius and Suess, 2004;Niemann et al., 2013). Fractures visible on seismic profiles often exceed 10 m in length (Gabrielsen et al., 1998). However, surface sediments may also feature smaller-scale, branched fracture networks (hereafter referred to as mini-fractures) which propagate from macro-fractures as the fluid pressure increases (Friedman, 1975;Briggs et al., 2011;Anders et al., 2014).

The role of small-scale fracture networks in routing methane upwards into the near-surface sediments is not well understood. In particular, the biogeochemical effects of mini-fractures in sediments with methane-dependent microbial communities is poorly constrained but is important for our understanding of how fracture networks influence microbial dynamics. Geochemically, fractures facilitate migration of deep fluids that are laden with electron donors from deeper sediments, which can then be used by sedimentary microbes as metabolic/bioenergetics substrates. To date, such mini-fractures have either been detected by X-ray images of cores under pressure (Riedel et al., 2006), or by the presence of macroscopic biofilms lining subseafloor fractures (Briggs et al., 2011). These biofilms were usually present at the sulfate-methane transition zone (SMTZ), where methane is oxidized by a consortium of methanotrophic archaea and sulfate-reducing bacteria mediating the anaerobic oxidation of methane (AOM) with sulfate as the terminal electron acceptor (Knittel and Boetius, 2009):

$$CH_4 + SO_4^{2-} \rightarrow HCO_3^- + HS^- + H_2O \hspace{4cm} \text{Eq. (1)}$$

In contrast to large scale transport pathways, mini-fractures are difficult to detect as they cannot be resolved with seismic tools (Emery and Myers, 1996;Gabrielsen et al., 1998), and may thus play an underappreciated but potentially important role in sediment methane dynamics, and the efficiency of the benthic microbial methane filter.

In this study, we report on the presence of a mini-fracture in the near-surface sediments of the active pockmark Lomvi, located on the Vestnesa Ridge (79°N, 6°E), west of the Svalbard archipelago. Using an interdisciplinary approach that combines geochemical and organic geochemical methods, we investigate the effects that such mini-fractures may impose on benthic methane dynamics and associated microbial communities. Our data show that mini-fractures can provide conduits for advective gas migration fostering AOM, but the moderate expression of AOM-associated biogeochemical signals along the mini-fracture at the Lomvi pockmark suggest a rather recent opening of this particular fracture.

2 Material and Methods

2.1 Study sites

Vestnesa Ridge is NW-SE trending, ~100 km long and, covered with ~1km thick contourite drifted sediments. Vestnesa Ridge features numerous pockmark structures (see a more detailed description of the geological setting in Plaza-Faverola et al. (2015) and Panieri et al. (2017)). This ridge is part of a submarine gas-hydrate system on the west Svalbard margin

(1200m water depth), where fluid and gas migration from deep hydrocarbon reservoirs towards the seafloor has potentially been ongoing since the early Pleistocene (Knies et al., 2018). Past investigations have shown that the ridge actively releases methane gas from the seafloor along the eastern segment of the structure (Bünz et al., 2012;Smith et al., 2014;Plaza-Faverola et al., 2015;Panieri et al., 2017), and seismic data suggest that seepage is related to intensive seabed faulting and rifting

5 (Plaza-Faverola et al., 2015). The eastern part of Vestnesa Ridge features the pockmarks Lunde and Lomvi (Fig. 1), both belonging to the most active structures known in the area (Bünz et al., 2012;Panieri et al., 2017). Pockmarks are morphological expressions of fluid/gas-eruptions from sediments, and are commonly observed in active hydrocarbon systems (Hovland et al., 2002). Pockmarks can be prominent in the seafloor bathymetry, ranging in shape from circular, crater-like edifices to "push-down" sediment features (Hovland et al., 2002). Enhanced reflections and "push-down" features

10 observed in the seismic transects of Lunde and Lomvi were interpreted as chimney structures containing free gas, which originate from beneath the bottom of gas hydrate stability zone (Bünz et al., 2012;Smith et al., 2014). Excessive pore pressure at the summit of this gas column fractured the sediments and led to the presence of free gas in the hydrate stability zone (Weinberger and Brown, 2006;Bünz et al., 2012).

2.2 Sample collection

We investigated three sediment cores from Vestnesa Ridge: two were collected by a multicorer (MC) during cruise CAGE15-2 with R/V Helmer Hanssen in 2015 (core Lomvi 893MC and core Lunde 886MC), and an additional push core (core Lomvi 008PC) was recovered with the remotely operated vehicle (ROV) Ægir about 80m away from core Lomvi

20 893MC during the P1606 cruise with R/V G.O.Sars in 2016 (Table 1). The MC system used during cruise CAGE15-2 can collect up to six parallel cores during every deployment, and a MISO (Multidisciplinary Instrumentation in Support of Oceanography, Woods Hole Oceanographic Institution) tow-cam was attached to the MC frame, allowing targeted video-controlled sampling (Panieri et al., 2015;2017). Among the six cores, one was subsampled for porewater analyses, and two adjacent cores were used for lipid biomarker and headspace gas analyses, respectively. The cores for porewater extraction

25 were used for X-ray analysis. Core Lomvi 893MC was collected at a site with bacterial mats around outcropping carbonate crusts at the Lomvi pockmark, whereas core Lunde 886MC was collected at a soft sediment site with patchy bacterial mats and tubeworms at the Lunde pockmark (Figs. 1 and 2). The push core Lomvi 008PC was recovered from a large patch of bacterial mat at the Lomvi pockmark. This core was only sampled for the analysis of porewater and lipid biomarkers (limited sample material impeded the analysis of the gas composition from Lomvi 008PC).

30 Immediately upon recovery, we subsampled the cores for subsequent gas, porewater and biomarker analyses. Details on headspace sampling and gas analysis in the multi cores were described in Panieri et al. (2017) and references therein. Briefly, 5 mL of bulk sediments were sampled into a 20 mL headspace glass vial, containing 5 mL of 1M NaOH and two glass beads. The gas analysis was performed with a ThermoScientific Trace 1310 gas chromatograph (GC) equipped with a TG-BOND alumnia (Na_2SO_4) column (30m×0.53 mm×10 μm). The methane headspace samples were obtained on a parallel

35 core as the fractured core in the same set of multicorer frame. Porewater was extracted at ambient temperature (ca. -1 °C), at a resolution of 2 cm, with either 10cm (Lomvi 893MC and Lunde 886MC) or 5 cm rhizon samplers (Lomvi 008PC) attached to acid-cleaned syringes (Seeberg-Elverfeldt et al., 2005). Rhizon membranes were soaked in Milli-Q water before use. The first 0.5 ml of the recovered porewater was discarded to avoid dilution/contamination with residual Milli-Q water in the rhizons. Sediment samples for biomarker analyses were collected onboard with a methanol pre-cleaned spatula at a

40 resolution of 2 cm, wrapped in aluminum foil and subsequently stored frozen at -20 °C until analysis. Intact sediment cores were kept at 4 °C for further X-ray analysis in onshore laboratories using a Geotek MSCL-XCT at UiT.

2.3 Porewater analyses

Total alkalinity (TA) was measured onboard using the Gran titration method (Grasshoff et al., 1999) within a few hours after the syringes were disconnected from the rhizon samplers. The HCl titrant (0.012M) was checked daily onboard with local surface seawater and 10mM borax to verify of the acid concentration. The pH meter of the titrator was calibrated with pH standard solutions (pH of 4, 7 and 11) both before and during the cruise. Porewater aliquots (2 ml) for sulfate analysis were preserved with 3 mL zinc acetate solution (23mM) to precipitate the dissolved sulfide (Gieske et al., 1991;Grasshoff et al., 1999) for CAGE 15-2 samples. All sulfate analyses were performed using a Dionex ICS-1100 Ion Chromatograph equipped with a Dionex IonPac AS23 column at Geological Survey of Norway (NGU) (Sauer et al., 2016). For sulfide concentration measurements, the precipitated zinc sulfide was quantified in the onshore geology laboratory at UiT with a spectrophotometric method (Cline, 1969) using a UV-1280 UV-vis Spectrophotometer (Shimadzu). The amount of zinc acetate added to samples from core 008PC was too low to precipitate all dissolved sulfide, thus the measured sulfide concentrations are minimum values. 2 mL aliquots of porewater were fixed onboard with saturated $HgCl_2$ (27mM final concentration) for the subsequent measurement of $\delta^{13}C$ of dissolved inorganic carbon (DIC) (Grasshoff et al., 1999). The $\delta^{13}C$-DIC of CAGE 15-2 samples (Bernhard and Panieri, 2018) were analyzed using a Finnigan DELTA-Plus mass spectrometer coupled to a Gas-Bench II as described in Torres et al. (2005). The $\delta^{13}C$-DIC in pore waters of core Lomvi 008PC was determined from the CO_2 liberated from the water after acidification with phosphoric acid. Measurements were carried out at EAWAG (The Swiss Federal Institute of Aquatic Science and Technology) using an IRMS (Isotope Ratio Mass Spectrometer, Isoprime) equipped with a Gilson 222XL Liquid Handler and a Multiflow unit (Isoprime). The standard deviation of the $\delta^{13}C$-DIC measurements from repeated measurements of standards was ±0.1‰ (1σ, n=27). The stable carbon isotope values for DIC are reported in the conventional δ-notation in permil (‰) relative to V-PDB (Vienna Pee Dee Belemnite).

2.4 Lipid extraction, quantification, identification and determination of compound-specific stable carbon isotope composition.

Lipid biomarkers were extracted and analyzed according to previously reported protocols (Elvert et al., 2003) with modification for alcohol derivatization (Niemann et al., 2005), and instrument set up (Blees et al., 2014;Steinle et al., 2018). Briefly, a total lipid extract (TLE) was obtained by ultrasonication of ~20g wet sediment samples in four extraction steps with solvents of decreasing polarity: dichloromethane (DCM)/methanol (MeOH) 1: 2; DCM/ MeOH 2: 1; and DCM for the last two extraction steps. The TLE was then saponified, and a neutral lipid fraction was extracted prior to methylation of the remaining polar fraction (comprising free fatty acids) to yield fatty acid methyl esters (FAME) for chromatographic analysis. Double bond positions of FAMEs were determined by analyzing dimethyl-disulfide adducts (Nichols et al., 1986; Moss and Lambert-Fair 1989). The neutral fraction was further separated into hydrocarbons, ketones, and alcohols, the latter of which was derivatized to form trimethylsilyl adducts for analysis.

Individual lipid compounds were analyzed using a GC (Thermo Scientific TRACE™ Ultra), equipped with a capillary column (Rxi-5ms, 50 m, 0.2 mm id, 0.33 µm df), using helium gas as a carrier gas at a constant flow rate of 1 mL min⁻¹. The initial oven temperature was set to 50 °C, held for 2 min and then increased to 140 °C at a rate of 10 °C min⁻¹, held for 1 min, then further increased to 300°C at 4 °C min⁻¹. The final hold time was 63 min to analyze FAMEs or 160 min to analyze larger (i.e., high boiling point) lipids in the hydrocarbon and alcohol fractions. Concentrations were determined by flame-ionization detection (FID) against internal standards. Unknown compounds were identified with a quadrupole mass spectrometry unit (Thermo Scientific DSQ II) at the chromatography periphery. Similarly, compound-specific stable carbon isotope ratios were determined using a magnetic sector isotope ratio mass spectrometry unit (Thermo Scientific Delta V

Advantage) coupled to a gas chromatography setup with the above-outlined specification. $\delta^{13}C$ values are reported with an analytical error of $\pm$ 1‰.

3 Results and Discussion

3.1 Sediment X-ray imaging and porewater geochemistry

Our detailed X-ray imaging of cores retrieved from locations of known methane seepage in the Vestnesa Ridge revealed a mini-fracture in the core Lomvi 893MC in the top 30 cm (Fig. 3) but not in any other core. However, it is important to note that X-ray imaging can only confirm the presence of a fracture while the size/expansion of the original fracture cannot be resolved. Upon recovery, core Lomvi 893MC showed extensive gas ebullition. Thus it is possible that the fracture expanded during core retrieval because of pressure-induced volume changes of sedimentary gases. Nevertheless, our analyses revealed a substantial increase of methane concentrations in the upper section of the core (Fig. 4), which is an uncommon observation in marine settings where methane originates at greater sediment depth (i.e., methane concentrations typically increase downcore). We argue that the higher concentration at the surface of the core directly indicate an advective (fracture controlled) influx of methane into the top sediment section at the coring side of the core Lomvi 893MC. Typically, high sediment methane concentrations in marine sediments lead to elevated rates of AOM, which in return lead to sulfate depletion and sulfide production, and thus the development of a sulfate methane transition zone (SMTZ). Furthermore, excess production of DIC during AOM leads to elevated sediment TA and low $\delta^{13}C$-DIC values. The marked methane increase at coring site Lomvi 893MC was not paralleled by changes in other parameters, which are commonly associated with AOM (Fig. 4a). Rather, the smooth porewater profiles of sulfate, sulfide, TA and $\delta^{13}C$ of DIC in this core seem typical for locations with low methane input, as often found in settings characterised by diffusive transport regimes (Treude et al., 2003;Egger et al., 2018;Niemann et al., 2009). We attribute this apparently contradictory observation of enhanced methane concentrations on the one hand and the rather 'inconspicuous' signals for AOM activity on the other to a recent genesis of the fracture (see additional discussion below). To further investigate the changes associated with the highly heterogeneous nature of the methane dynamics in this region, we compared this first core with two additional cores from contrasting settings at the Vestnesa Ridge.

The push core Lomvi 008PC retrieved from an active venting site (ca. 80 m to the SE of core Lomvi 893MC) at the Lomvi pockmark showed sulfate-depletion within the first 5 cmbsf (Fig. 4b), indicating a high methane flux and a shallow SMTZ (Reeburgh, 2007). This shallow SMTZ is comparable to those typically observed at locations of high methane flux, such as the *Beggiatoa* fields at Hydrate Ridge (Treude et al., 2003), the Gulf of Mexico (Ussler and Paull, 2008) or Haakon Mosby Mud Volcano (Niemann et al., 2006a, b) . At these high flux sites, AOM rates have been estimated to be in the order of several mmol m^{-2}d^{-1}. A third core (core Lunde 886MC) was retrieved from a soft-sediment site characterised by the extensive occurrence of tubeworms and bacterial mats (Fig. 2) at the adjacent active Lunde Pockmark. Sulfate concentrations in this core showed only a moderate decrease with sediment depth and trace methane was detected in the upper 20 cm of the core (Fig. 4c). These data are consistent with observations of low sulfide concentrations and TA. Together, our results indicate a substantially lower methane flux and efficient methane retention through AOM in sediments at this coring site similar to previous findings from seep sites characterised by macrofaunal inducing bioventilation e.g. Niemann et al., 2006a, b; Levin et al., 2016. Although core Lunde 886MC is located in a diffusive system, the convex shape of the sulfate concentration profile along with increasing methane concentration at the bottom suggest non-steady state conditions. The convex shape of the sulfate profile can be related to an ongoing increase in methane flux (Fischer et al., 2013;Hong et al.,

2017b). It may also be related to the intrusion of seawater into the shallower sediments, which can be induced by bioventilation, and/or ascending methane bubbles from the sub-seafloor (Haeckel et al., 2007;Hong et al., 2016). Our visual investigations of the seafloor revealed the presence of tubeworms but only few bivalves, therefore bioventilation would be moderate. Methane concentration in the upper sediment section was very low, and we did not observe methane bubbles emanating from the seafloor at the coring site. We thus assume that moderate bio-irrigation and a recent increase of the diffusive methane flux at the coring site (Lunde 886MC) can explain the non-steady state sulfate and methane profiles in the Lunde pockmark core.

3.2 Methanotrophic community development

To further investigate the role of the detected mini-fracture in core Lomvi 893MC on the biogeochemistry and microbial community, we investigated archaeal and bacterial lipid biomarkers and their associated stable carbon isotope signatures that are diagnostic for AOM communities (Niemann and Elvert 2008, and references therein). ANME typically produce a suite of glycerol ether lipids comprising isoprenoidal alkyl moieties that may also occur as free hydrocarbons in environmental samples. We found the isoprenoidal dialkyl glycerol diethers archaeol and *sn-2*-hydroxylarchaeol in all three cores (Fig. 4a-c). Furthermore, the ^{13}C-depleted signatures of these compounds provide evidence that their source organisms mediate sulfate-dependent AOM. Indeed, ANME biomass is characterized by a strongly ^{13}C-depleted isotope composition because the metabolized methane is typically ^{13}C-depleted, and AOM is associated with a strong kinetic isotope effect (Whiticar, 1999). The sulfate-reducing partner bacteria involved in AOM produce characteristic fatty acids (C16:1ω5c, and cyC17:0ω5,6) which we observed at relatively high concentrations (Fig. 4 a-c). As these bacteria incorporate ^{13}C-depleted DIC produced by the anaerobic methanotrophs (Wegener et al., 2008), their stable carbon isotope signature was also depleted in ^{13}C. The biomarker data are consistent with an active AOM microbial population at all Vestnesa Ridge sites.

Our data also show, however, clear differences in the abundance of AOM-derived lipids at the three investigated coring sites (Figs. 4a-c). To highlight these differences, we calculated average concentrations and the isotopic depletion of archaeol and fatty acid C16:1ω5c (i.e. typical ANME and associated SRB lipids) relative to source methane (Δδ^{13}C-values) and compared these values to a non-seeping reference site south of Svalbard (Yao et al., 2017) and a known high methane flux site at Hydrate Ridge (Elvert et al., 2005) (Fig. 5). We chose Hydrate Ridge as the high flux comparison site because the only other observation of a mini-fracture was documented from that location (Briggs et al., 2011). We found the lowest concentrations of the diagnostic lipids at the non-seeping reference site, followed by the core Lunde 886MC, the core Lomvi 893MC, the core Lomvi 008PC and finally the Hydrate Ridge core. The substantially higher concentration of AOM-derived lipids at the Lomvi (particular in core Lomvi 008PC) compared to the Lunde site (core Lunde 886MC) is consistent with the geochemical signals of AOM (e.g. sulfate, sulfide, δ^{13}C of DIC) in the respective cores. The differences in concentrations of diagnostic lipids suggest a high standing stock of AOM communities in core Lomvi 008PC, and a much lower one in the other two cores. AOM communities grow very slowly, with doubling times of several months (Nauhaus et al., 2007;Zhang et al., 2011;Timmers et al., 2015). A sudden increase in methane flux/concentrations in the sulfate-rich sediments comprising only a small initial standing stock of AOM microorganisms, may eventually lead to elevated AOM activity, but with a significant lag time of several months to years. Our biomarker data suggests that the methanotrophic community at coring site Lomvi 893MC was not well developed, indicating that the increase in methane concentrations at that site occurred rather recently, probably less than a few years prior to our sampling campaign. We found a more mature AOM community at the site Lomvi 008PC. Similarly, biofilms were observed to be associated with the mini-fracture at Hydrate Ridge (Briggs et al., 2011) indicate a more mature AOM community at this site. This suggests that the methane flux was higher at these sites for a longer period of time, allowing for the establishment of the slow-growing AOM community.

Because of the spatial dynamics of venting at the Lomvi pockmark in Vestnesa Ridge (Bohrmann et al., 2017;Hong et al., 2017ab;Panieri et al., 2017), it is likely that the biomarker results reflect the cumulative history of microbial AOM activity, rather than solely the most recent situation. Nonetheless, we observed a general decrease in $\delta^{13}C$ of both bacterial and archaeal lipids in horizons of present day sulfate depletion indicating a higher contribution of AOM-derived compounds to the lipid pool. Such decrease in $\delta^{13}C$ was apparent at ~10 cmbsf in Lomvi 893MC where sulfide started to accumulate, at ~5 cmbsf in core Lomvi 008PC where sulfate was depleted, and at 10-15 cmbsf in Lunde 886MC where methane began to increase downcore (Fig. 4). At these depths, the ratios of *sn*-2-hydroxylarchaeol to archaeol were 0.98 (core Lomvi 893MC), 0.37 (core Lomvi 008PC) and 0.26 (core Lunde 886MC), indicating ANME-1 as a likely key AOM organism at all the investigated coring sites (Niemann and Elvert, 2008). The known SRB types associated with ANME-1 and ANME-2 belong to the *Deltaproteobacteria, Desulfosarcina/Desulfococcus* clade Seep-SRB1, which typically display distinct ratios of the fatty acids C16:1ω5c relative to isoC15:0. In systems dominated by Seep-SRB1 associated to ANME-1 this value is commonly <2, while it is >>2 in systems where Seep-SRB-1 is associated with ANME-2 (Niemann and Elvert, 2008). At all coring locations, this biomarker ratio was >2 (3.2, core Lomvi 893MC; 5.4, core Lomvi 008PC; 7.9, core Lunde 886MC), which is indicative of an SRB eco type associated with ANME-2 rather than ANME-1. At this point, we can only speculate about these contradicting lipid patterns, and additional DNA-based tools would be needed to further identify the key AOM microbes at the investigated sites.

The ^{13}C-values of lipids from AOM communities are mainly influenced by isotope fractionation during AOM and the $\delta^{13}C$-value of the source methane-carbon (Summons et al., 1994, Riou et al., 2010), though other environmental parameters such as substrate availability and temperature are also known to influence lipid $\delta^{13}C$-signals. $\delta^{13}C$ -CH$_4$ values are typically low and the additional isotope fractionation during AOM reults in AOM-dereived lipid with $\delta^{13}C$ -values << -50 ‰. Our reference site showed $\delta^{13}C$ values of archaeal and bacterial lipids that were not conspicuously depleted. This indicates a low/negligible standing stock of AOM microbes at this site. Here, archaeal and bacterial lipids likely originated from processes other than AOM (e.g. organic matter degradation by heterotrophs). At site Lomvi 893MC, the $\delta^{13}C$ values of archaeal and bacterial lipids were not as negative as at the other three sites. The difference in the $\delta^{13}C$ signature of archaeol with respect to the source methane ($\delta^{13}C$-CH$_4$ = -57.8 ‰ in core Lomvi 893MC and -62.9 ‰ in core Lunde 886MC, Panieri et al. (2017)), were slightly lower in core Lomvi 893MC than in core Lunde 886MC (Fig. 5a). This may reflect an overprint from non-AOM related of lipids, which supports our assumption that the mini-fracture in core Lomvi 893MC and the associated AOM community developed rather recently. We do not know the source methane $\delta^{13}C$-value for core Lomvi 008PC, but assuming a uniform source methane value of -55 ‰ for the whole Lomvi pockmark area, then the highest $\Delta\delta^{13}C$ values were observed at Lomvi 008PC (Fig. 5). Together with the biomarker evidence for a significant AOM community and the rapid depletion of sulfate in this core, this indicates that AOM-biomass (and probably AOM activity) is more dominant at the Lomvi 008PC coring site than at the other two investigated sites. Although the AOM community seemed lower at Lunde 886MC, the $\Delta\delta^{13}C$ values were similar to the ones observed at Lomvi 008PC. This suggests that also here, despite the lower methane flux, AOM-communities dominated the overall microbial community.

Summary and conclusion

At the Lomvi pockmark, we found evidence for advective methane transport, with indication for different onsets of gas seepage at the different coring sites, while at the coring site at the Lunde pockmark, methane transport is dominated by diffusion (Fig. 6). Together with the porewater geochemical constrains, the distribution of ^{13}C-depleted lipid biomarker

underscores that the pockmark methane biogeochemistry is differentially affected by the advective vs. diffusive transport regimes. Our data show that high standing stocks of AOM communities thrive in surface sediments where methane concentrations are high, while in sediments where methane availability is limited, only a comparably low AOM biomass developed. The co-occurrence of a well-developed AOM standing stock and high CH_4 concentrations, however, cannot be considered a universal rule. Despite high methane concentrations in sediments featuring a mini-fracture, sediments contained a comparably low standing stock of AOM communities and geochemical signals for AOM activity were rather subtle. Methane transport through mini-fractures is advective and fractures thus represent important conduits for methane, facilitating the development of an active AOM community. Yet a high biomass of the slow-growing AOM communities require that advective transport has proceeded for an extended period of time after the onset of sediment fracturing (i.e., the development of AOM communities temporally lags behind). Our data suggest that the mini-fracture detected here opened rather recently, whereas methane transport at the other coring sites probably started much earlier. Mini-fractures are rarely recognized because they are below the resolution of seismic imaging tools and their detection is mostly incidental. Our study clearly highlights their relevance for benthic methane dynamics and adds to the very limited knowledge on the potential contribution of fracture-networks to benthic carbon cycling.

Data availability

All the data in the manuscript can be found in the supplementary materials.

Author contributions

H.Y. and G.P. collected biomarker samples, W-L. H., M.E.T., and S.S. contributed to porewater sampling and analyses. H.N. and M.F.L. supported lipid biomarker analyses. H.Y. wrote the majority of the manuscript. G.P and H.N. supervised the research. All authors contributed to the discussion of data and the writing of the paper at different stages.

Competing interests

We declare no conflict of competing interest for the co-authors.

Acknowledgements

We would like to acknowledge the captains, crews and all scientists on board R/V Helmer Hanssen cruise CAGE 15-2 and R/V G.O. Sars cruise P1606. We are especially thankful for Towcam operation by the team from Woods Hole Oceanographic Institution (WHOI) MISO (Multidisciplinary Instrumentation in Support of Oceanography) as well as ROV operation by the Ægir pilots. We would further like to thank Dr. Carsten J. Schubert and Serge Robert from EAWAG for the support during carbon isotopic analyses. This work was supported by the Research Council of Norway through its Centres of Excellence funding scheme (project number 223259). The publication charges for this article have been funded by a grant from the publication fund of UiT The Arctic University of Norway in Tromsø.

Table 1: Information of coring stations, coring coordinates, seafloor habitat information, analyses performed at each site. Abbreviations: DIC, dissolved inorganic carbon; TA, total alkalinity; conc, concentration.

Figure 1. Regional multibeam bathymetric map of Vestnesa Ridge showing the Lunde and Lomvi pockmarks and sampling locations. Locations of multicores and push cores used in this paper are denoted as red stars.

Figure 2. Still images of the seafloor before launching of the multicorer at coring site Lomvi 893MC (a) and coring site Lunde 886MC (c), as well as during ROV guided push coring at coring site Lomvi 008PC (b). Coring site Lomvi 893MC (a) and 008PC feature bacterial mats and reduced, black sediments, while the coring site Lunde 886MC (c) is characterised by soft sediments with tubeworms and small patchy bacterial mats. Green laser points (panel a, c) are 20 cm apart and the diameter of the push core (panel b) is 8.5 cm.

Figure 3. X-Ray images of core Lomvi 893MC. The different rotational planes show an whitish X-Ray transparency extending throughout the core. This zone is interpreted as a zone of weakness facilitating fluid and gas migration in situ. The void probably became gas filled after core recovery. Rotational video of this core is available in the supplementary materials.

Figure 4. Biogeochemical profiles of archaeal (*sn2*-hydroxyarchaeol, archaeol) and bacterial lipid biomarkers (fatty acids C16:1ω5c , cyC17:0 ω 5,6), methane and pore water constituents (sulfate, sulfide, DIC and total alkalinity) in the three cores Lomvi 893MC (a), Lomvi 008PC (b) and Lunde 886MC (c).

Figure 5. Average lipid biomarker concentrations and isotopic differences to source methane of the archaeal lipid archaeol ($\Delta\delta^{13}C$) (a, b) and the bacterial fatty acid C16:1ω5c (c, d). Cores Lomvi 893MC (averaged from 0-35cm), Lomvi 008PC (averaged from 0-33cm) and Lunde 886MC (averaged from 0-38cm) are compared to a high flux site at Hydrate Ridge (Elvert et al., 2005) and a core from a non-seeping site south of Svalbard (1522GC, 76.107°N, 15.957 °E, averaged from 0-350cm; (Yao et al., 2017).

Figure 6. Schematic illustration of different methane transport modes in the study area (big bubble and circle sizes highlight high methane concentrations and the approximate size of the standing stocks of AOM communities, respectively). Low amounts of methane in a diffusion dominated setting sustain a weakly defined AOM microbial community (right); mini-fracturing enhances the methane availability and fosters AOM community growth (left); the AOM community is fully developed after advective methane transport has continued for a longer period of time (middle).

Table 1. Investigated pockmark structures / coring sites

Pockmark (cruise)	Lomvi (CAGE15-2)	Lomvi (P1606)	Lunde (CAGE15-2)
Core	Lomvi 893MC	Lomvi 008PC	Lunde 886MC
Coordinates	79° 0.180′ N	79° 0.162′ N	79° 0.366′ N
	6° 55.434′ E	6° 55.488′ E	6° 54.030′ E
Habitat	bacterial mats and carbonate crusts	bacterial mats	tubeworms
Methane	methane headspace	N. A.	methane headspace
Porewater analyses	sulfate, sulfide, TA, δ^{13}C-DIC	sulfate, sulfide, TA, δ^{13}C-DIC	sulfate, sulfide, TA, δ^{13}C-DIC
Lipid biomarkers	conc. and δ^{13}C	conc. and δ^{13}C	conc. and δ^{13}C

Fig. 1.

Fig. 2.

Fig. 3.

Fig. 4.

(a) Lomvi 893 MC

(b) Lomvi 008 PC

(c) Lunde 886 MC

Fig. 5.

Δδ¹³C archaeol relative to source methane (‰)

Δδ¹³C C16:1ω5c relative to source methane (‰)

archaeol (µg.g⁻¹)

C16:1ω5c (µg.g⁻¹)
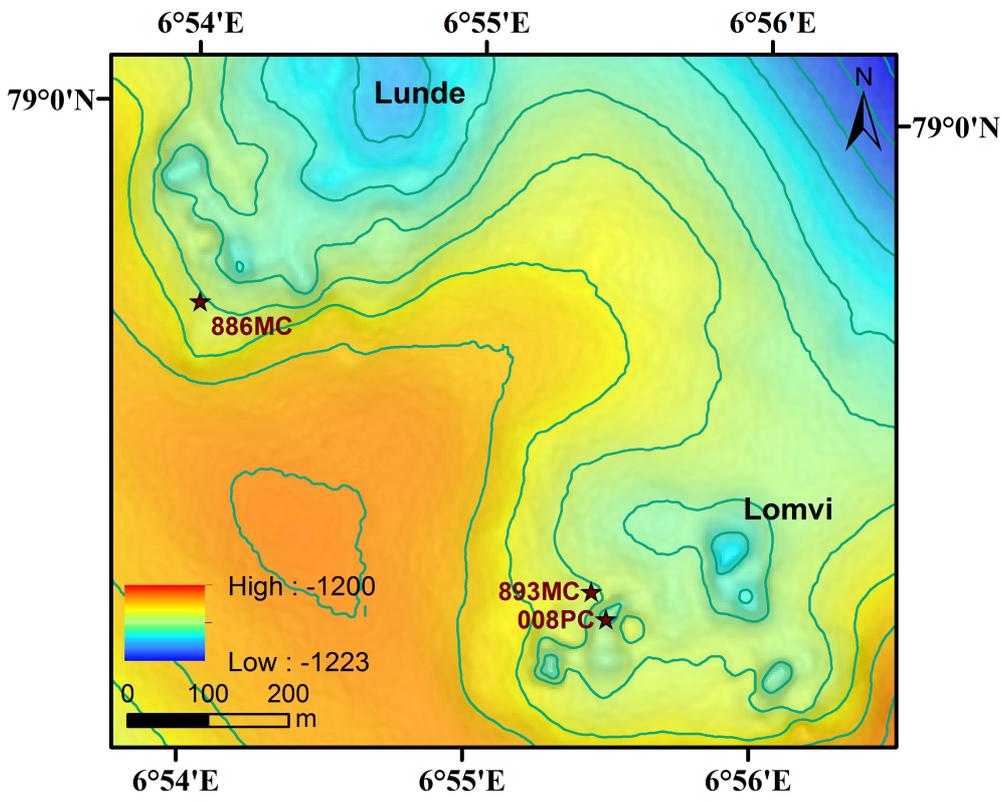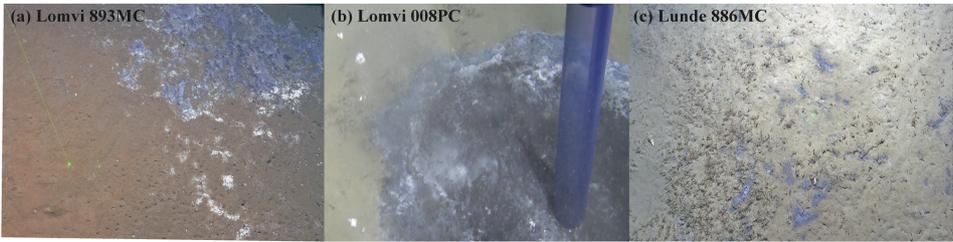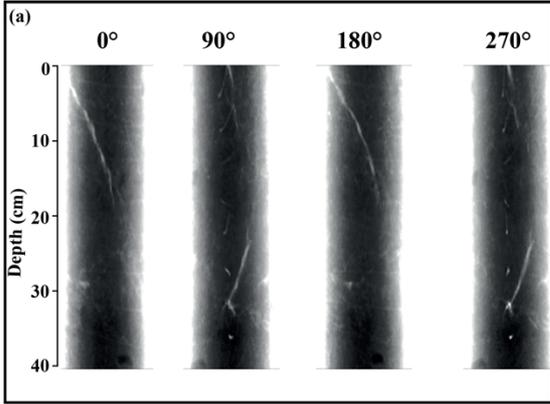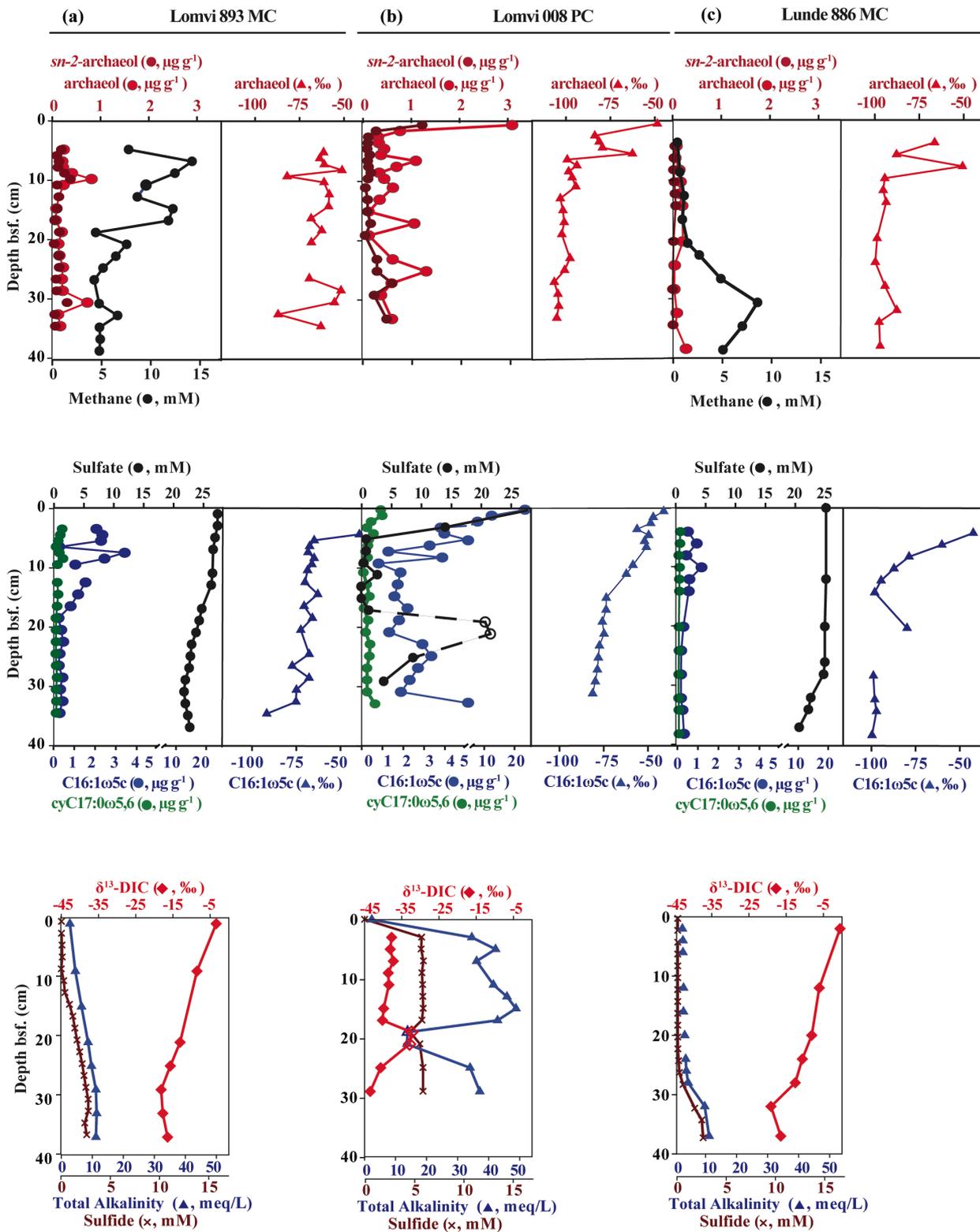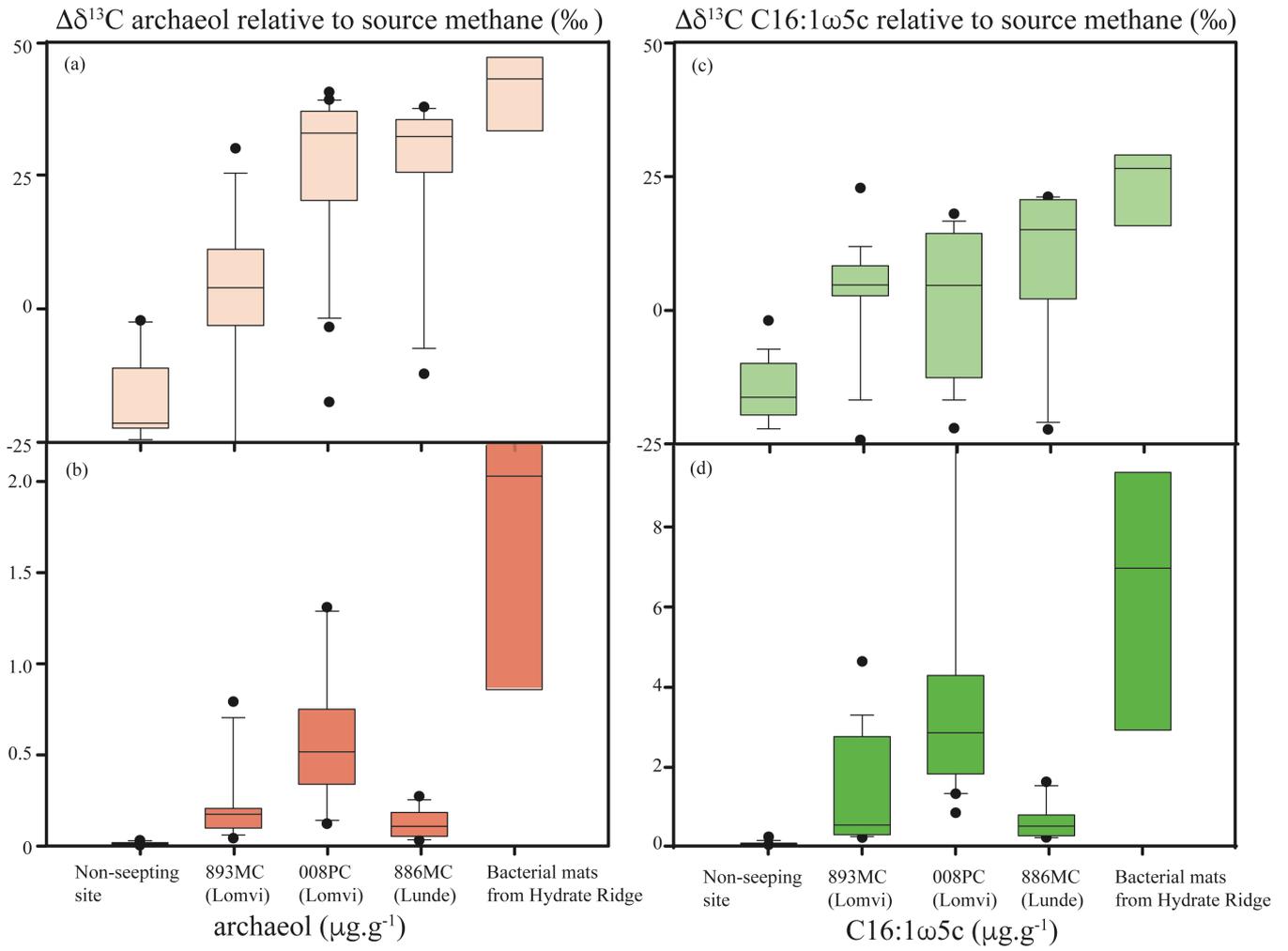
Fig. 6.
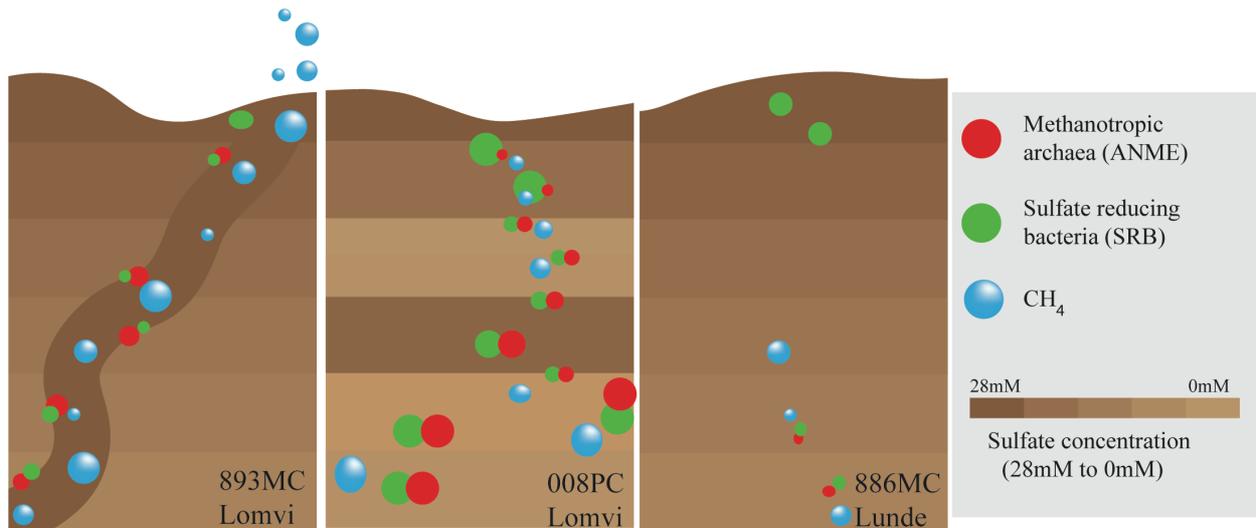
Reference

Anders, M. H., Laubach, S. E., and Scholz, C. H.: Microfractures: A review, Journal of Structural Geology, 69, 377-394, 10.1016/j.jsg.2014.05.011, 2014.

10   Berndt, C., Feseker, T., Treude, T., Krastel, S., Liebetrau, V., Niemann, H., Bertics, V. J., Dumke, I., Dunnbier, K., Ferre, B., Graves, C., Gross, F., Hissmann, K., Huhnerbach, V., Krause, S., Lieser, K., Schauer, J., and Steinle, L.: Temporal constraints on hydrate-controlled methane seepage off Svalbard, Science, 343, 284-287, 10.1126/science.1246298, 2014.

Bernhard, J. M., and Panieri, G.: Keystone Arctic paleoceanographic proxy association with putative methanotrophic bacteria, Sci Rep, 8, 10610, 10.1038/s41598-018-28871-3, 2018.

15   Blees, J., Niemann, H., Wenk, C. B., Zopfi, J., Schubert, C. J., Jenzer, J. S., Veronesi, M., and Lehman, M. F.: Bacterial methanotrophs drive the formation of a seasonal anoxic benthic nepheloid layer in an alpine lake, Limnology and Oceanography, 59, 1410-1420, 10.4319/lo.2014.59.4.141E, 2014.

Boetius, A., and Suess, E.: Hydrate Ridge: a natural laboratory for the study of microbial life fueled by methane from near-surface gas hydrates, Chemical Geology, 205, 291-310, 10.1016/j.chemgeo.2003.12.034, 2004.

20   Bohrmann, G., Ahrlich, F., Bergenthal, M., Bünz, S., Düßmann, R., Ferreira, C., Freudenthal, T., Fröhlich, S., Hamann, K., Hong, W.-L., Hsu, C., Johnson, J. E., Kaszemeik, K., Kausche, A., Klein, T., Lange, M., Lepland, A., Malnati, J., Meckel, S., Meyer-Schack, B., Noorlander, K., Panieri, G., Pape, T., Reuter, M., Riedel, M., Rosiak, U., Schmitdt, C., Schmidt, W.,

Seiter, C., Spagnoli, G., Stachowski, A., Stange, N., Wallmann, K., Wintersteller, P., Wunsch, D., and Yao, H.: R/V MARIA S. MERIAN Cruise Report MSM57, Gas Hydrate Dynamics at the Continental Margin of Svalbard, Reykjavik - Longyearbyen - Reykjavik, 29 July - 07 September 2016, MARUM – Zentrum für Marine Umweltwissenschaften, Fachbereich Geowissenschaften, Universität Bremen, 1-204, 2017.

5   Briggs, B. R., Pohlman, J. W., Torres, M., Riedel, M., Brodie, E. L., and Colwell, F. S.: Macroscopic biofilms in fracture-dominated sediment that anaerobically oxidize methane, Appl Environ Microbiol, 77, 6780-6787, 10.1128/AEM.00288-11, 2011.

Bünz, S., Polyanov, S., Vadakkepuliyambatta, S., Consolaro, C., and Mienert, J.: Active gas venting through hydrate-bearing sediments on the Vestnesa Ridge, offshore W-Svalbard, Marine Geology, 332-334, 189-197, 10   10.1016/j.margeo.2012.09.012, 2012.

Cline, J. D.: Spectrophotometric Determination of Hydrogen Sulfide in Natural Waters, Anal. Chem, 21, 1005-1009, 1969.

Egeberg, P. K., and Dickens, G. R.: Thermodynamic and pore water halogen constraints on gas hydrate distribution at ODP Site 997 Blake Ridge, Chemical Geology, 153, 53-79, 1999.

15   Egger, M., Riedinger, N., Mogollón, J. M., and Jørgensen, B. B.: Global diffusive fluxes of methane in marine sediments, Nature Geoscience, 11, 421-425, 10.1038/s41561-018-0122-8, 2018.

Elvert, M., Boetius, A., Knittel, K., and Jørgensen, B. B.: Characterization of Specific Membrane Fatty Acids as Chemotaxonomic Markers for Sulfate-Reducing Bacteria Involved in Anaerobic Oxidation of Methane, Geomicrobiology Journal, 20, 403-419, 10.1080/01490450303894, 2003.

20   Elvert, M., Hopmans, E. C., Treude, T., Boetius, A., and Suess, E.: Spatial variations of methanotrophic consortia at cold methane seeps: implications from a high-resolution molecular and isotopic approach
Geobiology, 3, 195-209, 2005.

Emery, D., and Myers, K. J.: Sequence Stratigraphy, Blackwell Science, Oxford, 1996.

Fischer, D., Mogollón, J. M., Strasser, M., Pape, T., Bohrmann, G., Fekete, N., Spiess, V., and Kasten, S.: Subduction zone 25   earthquake as potential trigger of submarine hydrocarbon seepage, Nature Geoscience, 6, 647-651, 10.1038/ngeo1886, 2013.

Friedman, M.: Fractur in Rock, Reviews of Geophysics and Space Physics, 13, 352-358, 1975.

Gabrielsen, R. H., Aarland, R.-K., and Alsaker, E.: Identification and spatial distribution of fractures in porous, siliclastic sediments., in: Structrual Geology in Reservoir Characterization, edited by: Coward, M. P., Daltaban, T. S., and Johnson, H., Geological Society, London, 49-64, 1998.

30   Gieske, J., Gamo, T., and Brumsack, H.: CHEMICAL METHODS FOR INTERSTITIAL WATER ANALYSIS ABOARD JOIDES RESOLUTION
OCEAN DRILLING PROGRAM TEXAS A&M UNIVERSITY Technical Note 15, 1991.

Grasshoff, K., Kremling, K., and Ehrhardt, M.: Methods of Seawater Analysis, Wiley-VCH, 1999.

Haeckel, M., Boudreau, B. P., and Wallmann, K.: Bubble-induced porewater mixing: A 3-D model for deep porewater 35   irrigation, Geochimica et Cosmochimica Acta, 71, 5135-5154, 10.1016/j.gca.2007.08.011, 2007.

Hong, W.-L., Sauer, S., Panieri, G., Ambrose, W. G., James, R. H., Plaza-Faverola, A., and Schneider, A.: Removal of methane through hydrological, microbial, and geochemical processes in the shallow sediments of pockmarks along eastern Vestnesa Ridge (Svalbard), Limnology and Oceanography, 61, S324-S343, 10.1002/lno.10299, 2016.

Hong, W.-L., Schmidt, C., Yao, H., Wallmann, K., Rae, J., Lepland, A., Torres, M., Plaza-Faverola, A., Latour, P., Bunz, S., and Bohrmann, G.: Fracture-Induced Fluid Migration in an Arctic Deep Water Pockmark: Porewater Geochemistry from the MEBO Drilling (MSM57) in Vestnesa Ridge (Svalbard), Goldschmidt Abstract, Paris, 2017a.

Hong, W. L., Torres, M. E., Carroll, J., Cremiere, A., Panieri, G., Yao, H., and Serov, P.: Seepage from an arctic shallow marine gas hydrate reservoir is insensitive to momentary ocean warming, Nat Commun, 8, 15745, 10.1038/ncomms15745, 2017b.

Hong, W. L., Torres, M. E., Portnov, A., Waage, M., Haley, B., and Lepland, A.: Variations in Gas and Water Pulses at an Arctic Seep: Fluid Sources and Methane Transport, Geophysical Research Letters, 10.1029/2018gl077309, 2018.

Hovland, M., Gardner, J. V., and Judd, A. G.: The significance of pockmarks to understanding fluid flow processes and geohazards, 2, 127-136, doi:10.1046/j.1468-8123.2002.00028.x, 2002.

Knies, J., Daszinnies, M., Plaza-Faverola, A., Chand, S., Sylta, Ø., Bünz, S., Johnson, J. E., Mattingsdal, R., and Mienert, J.: Modelling persistent methane seepage offshore western Svalbard since early Pleistocene, Marine and Petroleum Geology, 91, 800-811, 10.1016/j.marpetgeo.2018.01.020, 2018.

Knittel, K., and Boetius, A.: Anaerobic oxidation of methane: progress with an unknown process, Annu Rev Microbiol, 63, 311-334, 10.1146/annurev.micro.61.080706.093130, 2009.

Levin, L. A., Baco, A. R., Bowden, D. A., Colaco, A., Cordes, E. E., Cunha, M. R., Demopoulos, A. W. J., Gobin, J., Grupe, B. M., Le, J., Metaxas, A., Netburn, A. N., Rouse, G. W., Thurber, A. R., Tunnicliffe, V., Van Dover, C. L., Vanreusel, A., and Watling, L.: Hydrothermal Vents and Methane Seeps: Rethinking the Sphere of Influence, Frontiers in Marine Science, 3, 10.3389/fmars.2016.00072, 2016.

Nauhaus, K., Albrecht, M., Elvert, M., Boetius, A., and Widdel, F.: In vitro cell growth of marine archaeal-bacterial consortia during anaerobic oxidation of methane with sulfate, Environ Microbiol, 9, 187-196, 10.1111/j.1462-2920.2006.01127.x, 2007.

Niemann, H., Elvert, M., Hovland, M., Orcutt, B., Judd, A., Suck, I., Gutt, J., Joye, S., Damm, E., Finster, K., and Boetius, A.: Methane emission and consumption at a North Sea gas seep (Tommeliten area), Biogeosciences, 2, 335-351, 2005.

Niemann, H., Duarte, J., Hensen, C., Omoregie, E., Magalhães, V. H., Elvert, M., Pinheiro, L. M., Kopf, A., and Boetius, A.: Microbial methane turnover at mud volcanoes of the Gulf of Cadiz, Geochimica et Cosmochimica Acta, 70, 5336-5355, 10.1016/j.gca.2006.08.010, 2006a.

Niemann, H., Losekann, T., de Beer, D., Elvert, M., Nadalig, T., Knittel, K., Amann, R., Sauter, E. J., Schluter, M., Klages, M., Foucher, J. P., and Boetius, A.: Novel microbial communities of the Haakon Mosby mud volcano and their role as a methane sink, Nature, 443, 854-858, 10.1038/nature05227, 2006b.

Niemann, H., and Elvert, M.: Diagnostic lipid biomarker and stable carbon isotope signatures of microbial communities mediating the anaerobic oxidation of methane with sulphate, Organic Geochemistry, 39, 1668-1677, 10.1016/j.orggeochem.2007.11.003, 2008.

Niemann, H., Fischer, D., Graffe, D., Knittel, K., Montiel, A., Heilmayer, O., Nothen, K., Pape, T., Kasten, S., Bohrmann, G., Boetius, A., and Gutt, J.: Biogeochemistry of a low-activity cold seep in the Larsen B area, western Weddell Sea, Antarctica, Biogeosciences, 6, 2383-2395, 10.1594/PANGAEA.702077, 2009.

Niemann, H., Linke, P., Knittel, K., MacPherson, E., Boetius, A., Bruckmann, W., Larvik, G., Wallmann, K., Schacht, U., Omoregie, E., Hilton, D., Brown, K., and Rehder, G.: Methane-carbon flow into the benthic food web at cold seeps--a case study from the Costa Rica subduction zone, PLoS One, 8, e74894, 10.1371/journal.pone.0074894, 2013.

Panieri, G., Fornari, D. J., Serov, P., Astrom, E. K. L., Plaza-Faverola, A., Mienert, J., and Torres, M.: Gas hydrate, carbonate cruists, and chemosynthetic organisms on Vestnesa Ridge Pockmark- Preliminary findings., Fire in the ice, 15, 14-17, 2015.

Panieri, G., Bünz, S., Fornari, D. J., Escartin, J., Serov, P., Jansson, P., Torres, M. E., Johnson, J. E., Hong, W., Sauer, S., Garcia, R., and Gracias, N.: An integrated view of the methane system in the pockmarks at Vestnesa Ridge, 79°N, Marine Geology, 390, 282-300, 10.1016/j.margeo.2017.06.006, 2017.

Plaza-Faverola, A., Bünz, S., Johnson, J. E., Chand, S., Knies, J., Mienert, J., and Franek, P.: Role of tectonic stress in seepage evolution along the gas hydrate-charged Vestnesa Ridge, Fram Strait, Geophysical Research Letters, 42, 733-742, 10.1002/2014gl062474, 2015.

Reeburgh, W. S.: Oceanic Methane Biogeochemistry, Chem. Rev, 107, 486-513, 2007.

Riedel, M., Collett, T. S., Malone, M. J., and scientists, t. E.: Site U1328, in: Proceedings of the IODP, 311, Proceedings of the IODP, 2006.

Sahling, H., Römer, M., Pape, T., Bergès, B., dos Santos Fereirra, C., Boelmann, J., Geprägs, P., Tomczyk, M., Nowald, N., Dimmler, W., Schroedter, L., Glockzin, M., and Bohrmann, G.: Gas emissions at the continental margin west of Svalbard: mapping, sampling, and quantification, Biogeosciences, 11, 6029-6046, 10.5194/bg-11-6029-2014, 2014.

Sauer, S., Hong, W.-L., Knies, J., Lepland, A., Forwick, M., Klug, M., Eichinger, F., Baranwal, S., Crémière, A., Chand, S., and Schubert, C. J.: Sources and turnover of organic carbon and methane in fjord and shelf sediments off northern Norway, Geochemistry, Geophysics, Geosystems, 17, 4011-4031, 10.1002/2016gc006296, 2016.

Seeberg-Elverfeldt, J., Schluter, M., Feseker, T., and Kolling, M.: Rhizon sampling of porewaters near the sediment-water interface of aquatic systems, Limnology and Oceanography, 3, 361-371, 2005.

Smith, A. J., Mienert, J., Bunz, S., and Greinert, J.: Thermogenic methane injection via bubble transport into the upper Arctic Ocean from the hydrate-charged Vestnesa Ridge, Svalbard, Geochemistry, Geophysics, Geosystems, 15, 1945–1959, 10.1002/, 2014.

Steinle, L., Knittel, K., Felber, N., Casalino, C., de Lange, G., Tessarolo, C., Stadnitskaia, A., Sinninghe Damsté, J. S., Zopfi, J., Lehmann, M. F., Treude, T., and Niemann, H.: Life on the edge: active microbial communities in the Kryos MgCl2-brine basin at very low water activity, The ISME Journal, 12, 1414-1426, 10.1038/s41396-018-0107-z, 2018.

Timmers, P. H., Gieteling, J., Widjaja-Greefkes, H. C., Plugge, C. M., Stams, A. J., Lens, P. N., and Meulepas, R. J.: Growth of anaerobic methane-oxidizing archaea and sulfate-reducing bacteria in a high-pressure membrane capsule bioreactor, Appl Environ Microbiol, 81, 1286-1296, 10.1128/AEM.03255-14, 2015.

Tobin, H., Vannucchi, P., and Meschede, M.: Structure, inferred mechanical properties, and implications for fluid transport in the décollement zone, Costa Rica convergent margin, Geology, 29, 907-910, 10.1130/0091-7613(2001)029<0907:SIMPAI>2.0.CO;2, 2001.

Torres, M. E., McManus, J., Hammond, D. E., De Angelis, M. A., Heeschen, K. U., Colbert, S. L., Tryon, M. D., Brown, K. M., and Suess, E.: Fluid and chemical £uxes in and out of sediments hosting methane hydrate deposits on Hydrate Ridge, OR, I: Hydrological provinces, Earth and Planetary Science Letters, 201, 525-540, 2002.

Torres, M. E., Mix, A. C., and Rugh, W. D.: Precise δ13C analysis of dissolved inorganic carbon in natural waters using automated headspace sampling and continuous flow mass spectrometry, Limnology and Oceanography: Methods, 3, 349-360, doi:10.4319/lom.2005.3.349, 2005.

Treude, T., Boetius, A., Knittel, K., Wallmann, K., xf, and rgensen, B. B.: Anaerobic oxidation of methane above gas hydrates at Hydrate Ridge, NE Pacific Ocean, Marine Ecology Progress Series, 264, 1-14, 2003.

Ussler, W., and Paull, C. K.: Rates of anaerobic oxidation of methane and authigenic carbonate mineralization in methane-rich deep-sea sediments inferred from models and geochemical profiles, Earth and Planetary Science Letters, 266, 271-287, 10.1016/j.epsl.2007.10.056, 2008.

Waage, M., Portnov, A., Serov, P., Bünz, S., Waghorn, K. A., Vadakkepuliyambatta, S., Mienert, J., and Andreassen, K.: Geological Controls on Fluid Flow and Gas Hydrate Pingo Development on the Barents Sea Margin, Geochemistry, Geophysics, Geosystems, 20, doi:10.1029/2018GC007930, 2019.

Wegener, G., Niemann, H., Elvert, M., Hinrichs, K. U., and Boetius, A.: Assimilation of methane and inorganic carbon by microbial communities mediating the anaerobic oxidation of methane, Environmental Microbiology, 10, 2287–2298, 2008.

Weinberger, J., and Brown, K.: Fracture networks and hydrate distribution at Hydrate Ridge, Oregon, Earth and Planetary Science Letters, 245, 123-136, 10.1016/j.epsl.2006.03.012, 2006.

Whiticar, M.: Carbon and hydrogen isotope systematics of bacterial formation and oxidation of methane, Chemical Geology 161, 291-314, 1999.

Yao, H., Panieri, G., Knies, J., Belt, S. T., Koseoglu, D., and Niemann, H.: Past Methane Emissions in the Storfjordrenna Gas Hydrate-Bearing Mounds, Goldschmidt Abstract, Paris, 2017.

Zhang, Y., Maignien, L., Zhao, X., Wang, F., and Boon, N.: Enrichment of a microbial community performing anaerobic oxidation of methane in a continuous high-pressure bioreactor, BMC Microbiology, 11, 137, 10.1186/1471-2180-11-137, 2011.